Young Stellar Objects in the Low-Metallicity Small Magellanic Cloud

M. Sewiło (Johns Hopkins Univ., Space Science Institute), L. R. Carlson (Leiden Observatory), J. P. Seale (STScI), R. Indebetouw (Univ. of Virginia), M. Meixner (STScI), B. Whitney (Univ. of Wisconsin, Space Science Institute), T. P. Robitaille (MPIA), J. M. Oliveira (Keele Univ.), K. Gordon (STScI)

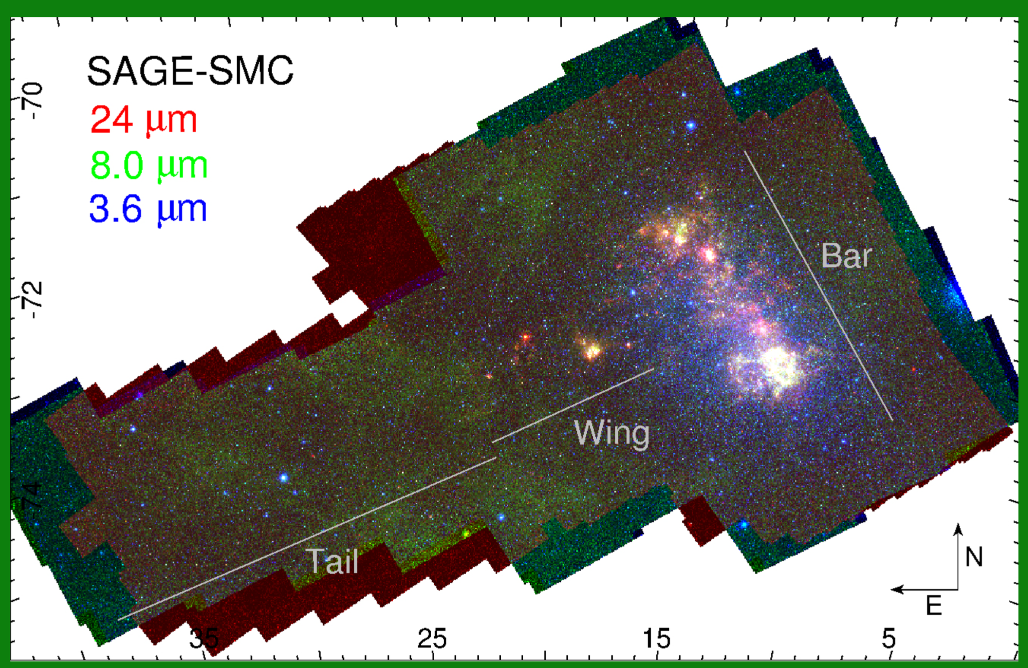

Figure 1: The SMC infrared view from the SAGE-SMC observations.

Abstract

The Small Magellanic Cloud offers unique opportunities to study star formation in a low-metallicity environment on galactic scales and within individual star-forming regions, clouds, and clusters. The proximity of the SMC (~60 kpc) makes it an ideal place for such studies without the confusion and extinction of the Galactic plane. The *Spitzer* Legacy Program ``Surveying the Agents of Galaxy Evolution in the Tidally-Stripped, Low-Metallicity Small Magellanic Cloud" (SAGE-SMC; Gordon et al. 2011) allows a global study of star formation in the SMC at high enough resolution to resolve individual cores and protostars at a range of mid-IR wavelengths.

Using the SAGE-SMC IRAC (3.6 - 8.0 µm) and MIPS (24 and 70 µm) catalogs and images combined with the near-IR and optical data, we identified a population of ~1000 intermediate- to high-mass Young Stellar Objects (YSOs) in the SMC (3x more than previously known). We investigate the properties of the YSOs and how they relate to the galaxy's structure and gas and dust distribution.

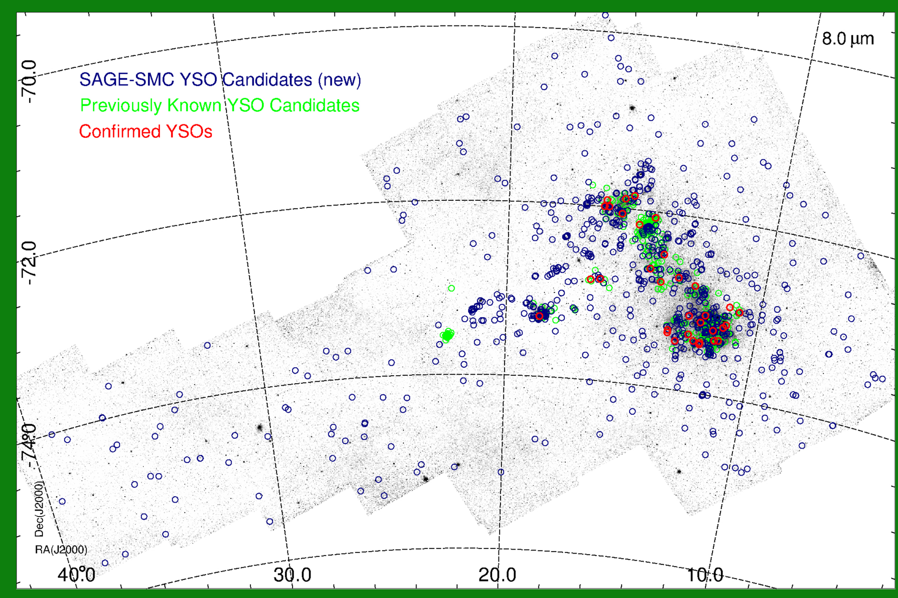

Figure 2: The distribution of newly discovered YSO candidates, along with previously known YSO candidates (~300 also present in the SAGE-SMC sample) and confirmed YSOs.

The YSO Identification

The method of identifying YSO candidates used in this work is based on a combination of successful methods developed by Whitney, Sewiło, et al. (2008), Gruendl & Chu (2009), and Sewiło et al. (2010) to search for the YSO candidates in the Large Magellanic Cloud. Additional modifications were made to further improve the YSO identification process.

The data:
* SAGE-SMC photometry: catalog when available; aperture photometry fill in missing bands
* Ancillary data: *JHKs* from 2MASS and IRSF
  optical data from MCPS (*UBVI*) and OGLE-III (*VI*)
* near- and mid-IR images

(1) Color-magnitude selection criteria
based on 5 CMDs combining all IRAC and MIPS 24 µm bands; select bright sources

Figure 3: An example CMD: the distribution of the SAGE-SMC catalog sources (in greyscale) is compared to the position of evolved stars (*left*), young stars (*middle*), and the YSO models (*right*). The region redward of the blue line was selected.

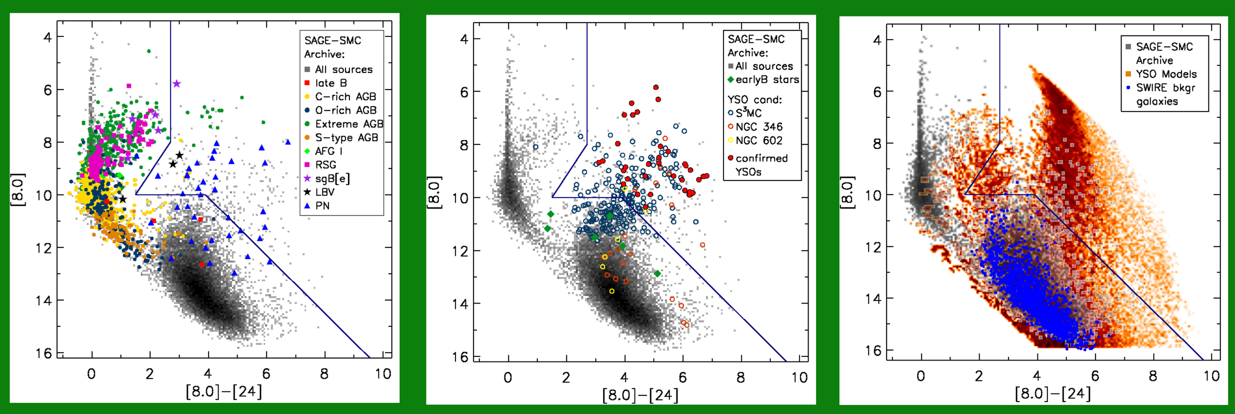

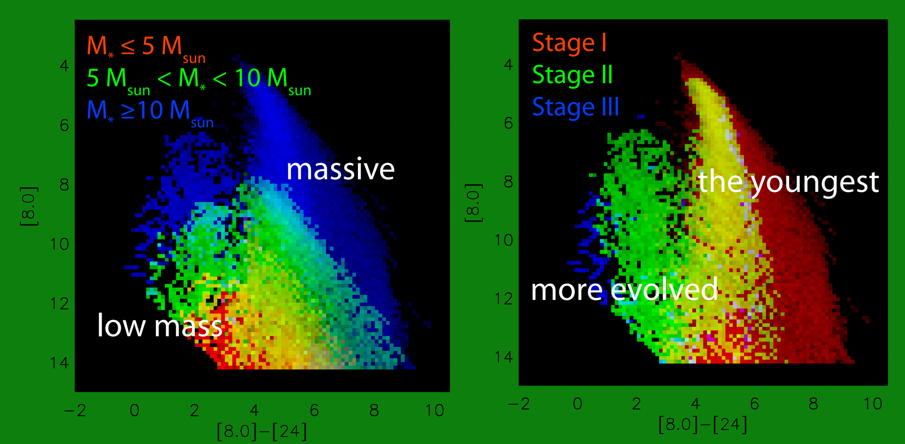

Figure 4: CMDs (the same as above) from a grid of YSO models scaled to standard IMF and SAGE-SMC sensitivity limits. Three colors represent three mass ranges (*left*) and three stages of evolution (*right*) as indicated in the legends.

The models show, that due to our selection criteria that avoided regions occupied by the galaxies and evolved stars, our YSO list is biased towards younger evolutionary stages and intermediate to high mass.

(2) Inspection of color-selected sources

We carefully examined the environment of the sources at all available images simultaneously with their spectral energy distributions (SEDs), and their location in the CMDs. We removed sources with non-YSO characteristics, unreliable sources, and objects morphologically identified as background galaxies.

(3) SED fitting with the YSO models using the model grid (~200,000 pre-computed 2-D YSO models; Robitaille et al. 2006). From the YSO model fits, we estimate stellar masses, luminosities, envelope infall rates, and disk masses.

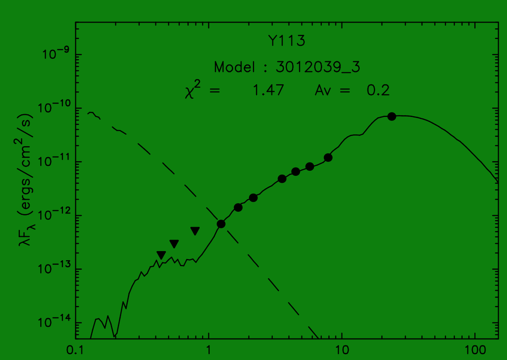

Figure 5: Example SED with the best YSO model fit (a solid line) for a young, spectroscopically confirmed protostar (Stage I YSO; $M_* \sim 15\ M_{sun}$). The dashed line is the central stellar atmosphere corresponding to the best fit model, extincted by the fitted foreground extinction. Filled circles and triangles are valid flux values and flux upper limits, respectively.

Final list: ~1000 YSO candidates

YSO Scores

For each YSO candidate, we calculated a measure of our confidence that the source is a YSO; we call this measure the YSO's ``CMD score". The CMD score ranges from 0 to ~4, with higher numbers signifying a greater confidence that the source is a YSO. The score is calculated based on where the source is located in the color-magnitude space with respect to the evolved stars, galaxies, and massive stars (in the CMDs used for the source selection), and scaled by a fraction of CMDs that can be constructed based on the source's photometry. We are more certain of the classification of the source that has more photometric measurements since we can gather more evidence by inspecting its location in more CMDs. Our YSO score calculation is a means of quantifying the varying certainties in YSO classification without the use of multiple inspections by a number of people.

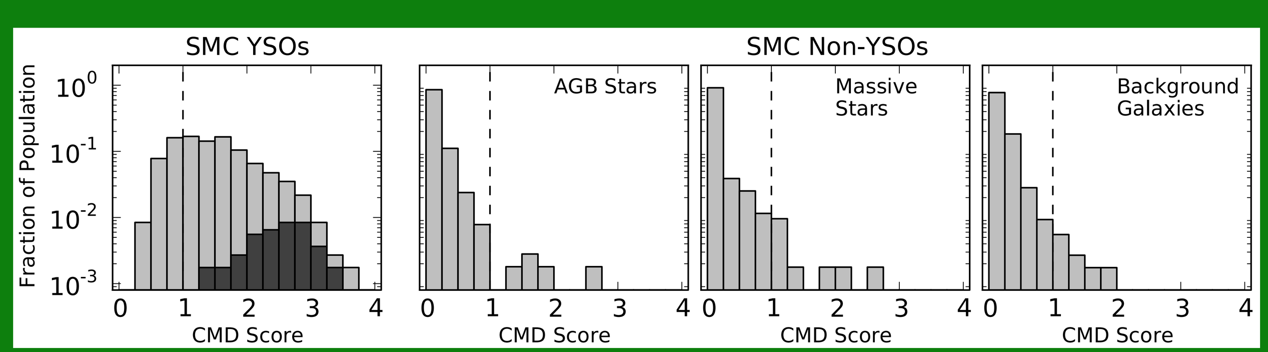

Figure 6: A comparison between the distribution of ``CMD scores" for the SAGE-SMC YSO candidates (*leftmost plot*) and scores of non-YSO populations (*from left to right*): evolved stars, massive stars, and background galaxies. The spectroscopically confirmed YSOs are shown in dark gray in the first plot on the left.

* As expected, the score distributions of non-YSO populations peak at lower scores than the distribution of scores of the YSO candidates and spectroscopically confirmed YSOs.
* The approximate separation between YSO candidates and non-YSOs occurs at the CMD score of 1 indicated by a vertical dashed line.

High-Reliability and Probable YSO Candidates

Based on scores and the results of the SED fitting, we define two classes of candidate YSOs:

High-reliability YSOs (~728):
* all sources with high scores (>1); good or bad (due to PAHs, variability, bad data points, etc.) YSO fits
* sources with low scores, but well-fitted with the YSO models

Probable YSOs (~262):
* low-score sources with no good YSO fits

Star Formation Rate in the SMC

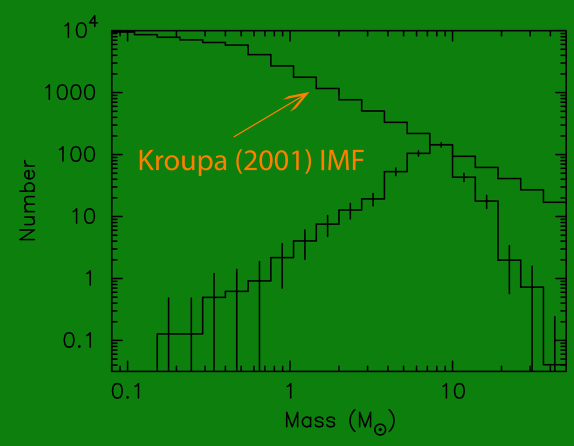

Figure 7: The distribution of stellar mass for high-reliability Stage I YSO candidates.

* attach Kroupa (2001) IMF to the mass function over the narrow range where the source list may be complete (Fig. 7; for Stage I YSOs)
* estimate total mass of Stage I YSOs by integrating Kroupa (2001) IMF
* calculate SFR for a range of lifetimes: from 0.07 Myr (high-luminosity sources) to 0.54 Myr (lower-luminosity sources); assume a constant star formation over these lifetimes
* the current SFR ~ total mass of YSOs over a lifetime

SFR: from ~0.058 to ~0.45 M_{sun}/yr

in good agreement with previous measurements at the low end:
~0.05 M_{sun}/yr (far-IR; W04)
~0.037 M_{sun}/yr (Hα + 24 microns; B11)

The YSO Candidates are spatially correlated with the gas tracers.

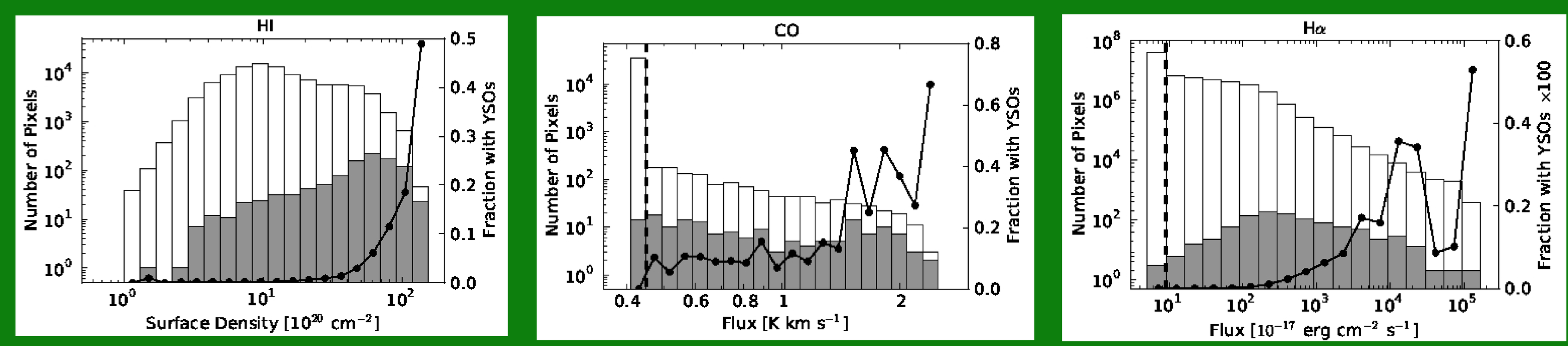

Figure 8: Pixel value histograms of the H I (*left*; S99), CO (*middle*; NANTEN), and Hα (*right*; MCELS) images. In each plot, the histogram shown in white includes pixels from the entire image (except areas outside the IRAC coverage in case of H I and Hα), while the gray color indicates pixels at the location of the YSO candidates. Black dots are the result of the division of the gray histogram by the white histogram and indicate a fraction of pixels associated with YSOs in each bin. The 3-sigma sensitivity of the image is marked with a vertical dashed line. The histograms show that YSO candidates are preferentially located in the regions of high H I column densities and high CO and Hα intensities.

Two Populations of YSO Candidates

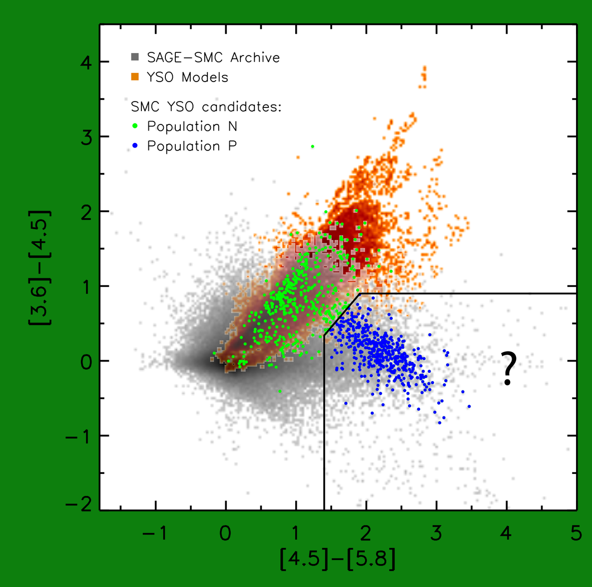

Figure 9: The CCD showing the distribution of the YSO candidates with respect to the R06 YSO models. The solid line shows a boundary between Population N and Population P sources.

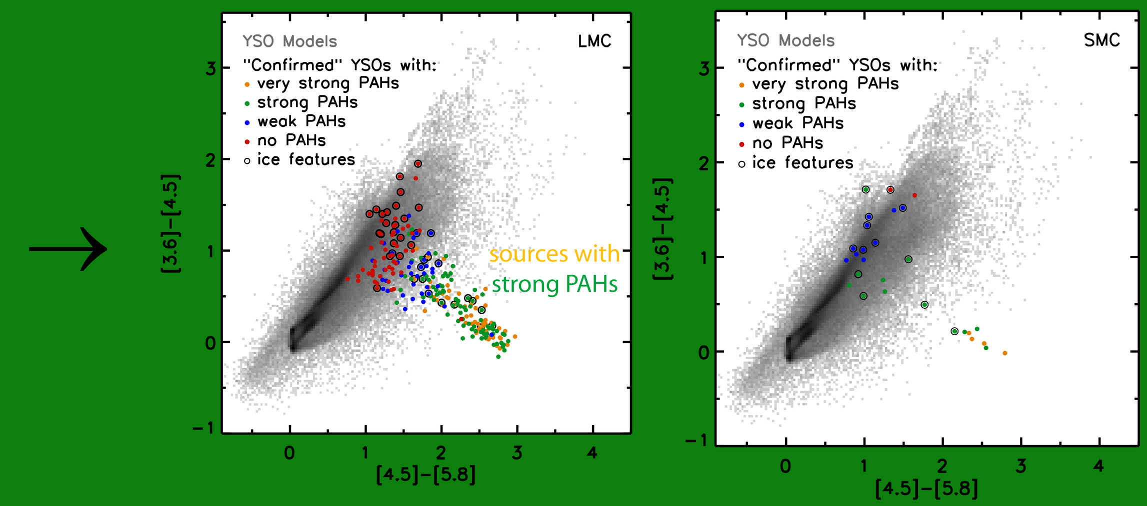

Figure 10: Spectroscopically confirmed YSOs in the LMC (left; S09) and SMC (right; O13) as a function of the strength of the polycyclic aromatic hydrocarbon (PAH) features. The Pop. N sources show no or weak PAH emission, while the Pop. P sources have strong PAH features in their spectra.

Pop. P does not overlap with the current YSO models that do not incorporate PAHs.

PAH Features in *Spitzer* IRAC Bands

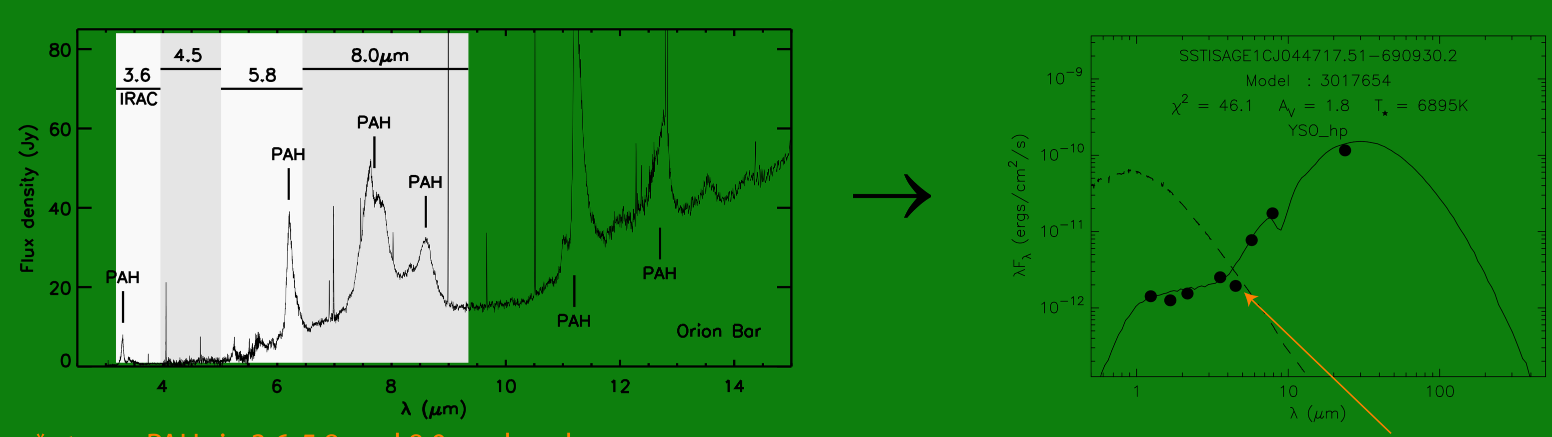

* strong PAHs in 3.6, 5.8, and 8.0 µm bands
* no PAHs in the 4.5 µm band --> sources become redder in [4.5]-[5.8] and are selected by our color-magnitude criteria

an example SED with the 4.5 µm ``dip" - the result of PAH enhancement at other IRAC bands

Population P: YSOs?

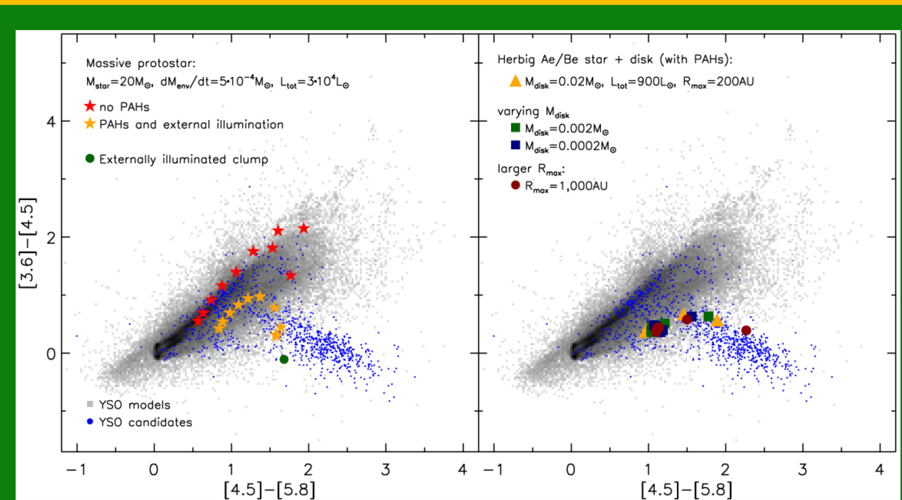

We examine the possibility that PAH emission could be causing the colors that were not predicted by our previous YSO models.

Figure 11 shows 2D radiative transfer models of the protostar with and without PAHs, and a model (with PAHs) of the Herbig Ae/Be star with disk. The models that take into account PAH emission also assume an external illumination (Whitney et al. 2013). The Herbig Ae/Be star models are shown for varying mass of the disk and outer radii. The models overlap with Pop. P.

Population P: Massive Main-Sequence Stars?

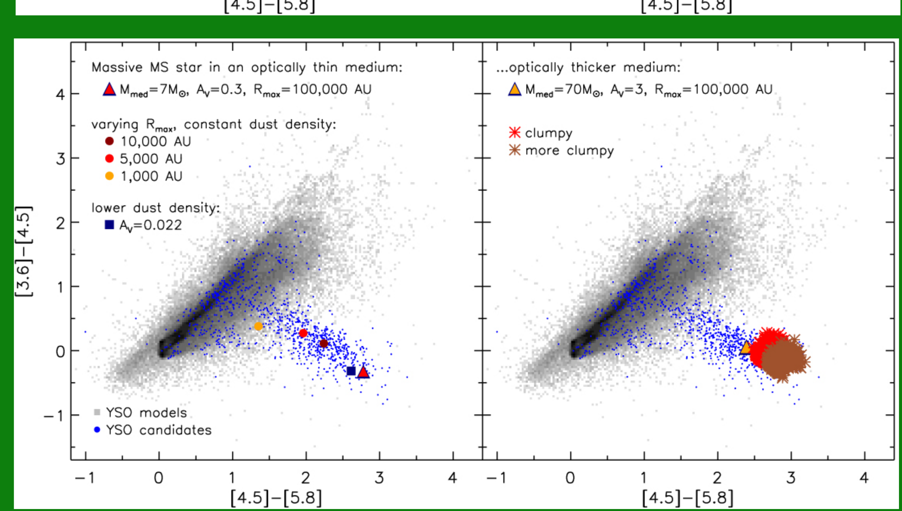

Population P can be contaminated by massive Main-Sequence (MS) stars illuminating nearby dust and exciting PAHs.

Figure 12 shows several massive MS star models with envelopes (molecular clouds or H II regions) of varying density, outer radii, and clumpiness. These models overlap with Pop. P. Some of the known OB stars (B10) lie in this area of the color-color space.

Follow-up spectroscopic observations are needed to distinguish between YSOs and massive MS stars.

References:
Bolatto, A., et al. 2011, ApJ, 74, 12
Bonanos, A. Z., et al. 2010, AJ, 140, 416
Fukui, Y., & Kawamura, A. 2010, ARA&A, 48, 547 (NANTEN)
Gordon, K., et al. 2011, AJ, 142, 102 (SAGE-SMC)
Gruendl, R., & Chu, Y.-H. 2009, ApJS, 184, 172
Kato, D., et al. 2007, PASJ, 59, 615 (IRSF Catalog)
Oliveira, J., et al. 2013, MNRAS, 428, 3001
Robitaille, T. P., et al. 2006, ApJS, 167, 256 (SED models)
Robitaille, T. P., et al. 2007, ApJS, 169, 328 (SED fitter)
Seale, J. P., et al., 2009, ApJ, 699, 150
Sewilo, M., et al. 2010, A&A, 518, 73
Stanimirovic, S., et al. 1999, MNRAS, 302, 417 (HI)
Udalski, A., et al. 2008, Acta Astron., 58, 329 (OGLE-III)
Wilke, K., et al. 2004, A&A, 414, 69
Whitney, B. A., Sewilo, M., et al. 2008, AJ, 136, 18
Whitney, B. A., Robitaille, T. P., et al. 2013, arXiv:1307.0561
Zaritsky, D., et al. 2002, AJ, 123, 855 (MCPS catalog)
The Hα image is provided by F. Winkler, S. D. Points, R. C. Smith, and the MCELS Team and NOAO/AURA/NSF